

EXPERIMENTAL EVIDENCE OF LOW SALINITY WATER FLOODING YIELDING A MORE OIL-WET BEHAVIOUR

Sandengen*, K., Tweheyo, M.T., Røphaug, M., Kjølhamar, A., Crescente, C., Kippe, V.
Statoil

This paper was prepared for presentation at the International Symposium of the Society of Core Analysts held in Austin, Texas, USA 18-21 September, 2011

ABSTRACT

Several research groups have shown that injection of low saline water may result in a wettability alteration towards a more water-wet behaviour. The present work shows a core flooding series where the response to low saline water injection was interpreted as yielding more oil-wetting conditions. Interpretation of secondary injection of both high-salinity and low-salinity water indicated a more oil-wet behaviour at low salinity. Using the relative permeability and capillary pressure data derived from these experiments, predictions of a tertiary mode low salinity injection experiment were in good qualitative agreement with experimental data. An ion exchange framework has been used to explain why such a wettability alteration is plausible for the present system.

The ion exchange mechanism has been reviewed to show how it can explain wettability alteration in both directions; either more oil-wetting or more water-wetting, depending on the oil and rock properties. A pH increase acts in the opposite direction than a decreased salinity. The latter may lead to artefacts in low pressure core floods and a simple CO₂ buffer system has been proposed as a convenient method to eliminate this pH uncertainty.

INTRODUCTION

In most experimental investigations low salinity injection has been interpreted as altering wettability towards a more water-wet behaviour. Ligthelm et.al. [1] provides a good overview of such laboratory observations as well as how an increased water-wetness relates to increased field recovery. When clays are present in the rock, ion exchange will inevitably occur when water composition changes. Lager et.al. [2] proposed that cation exchange yields a more water-wet surface due to desorption of organo-metallic complexes.

The contribution of the present work is threefold;

- To present an experimental series where the response to low salinity flooding was interpreted as a wettability alteration towards more oil-wetting conditions.

* Corresponding author, krian@statoil.com, Statoil R&D centre, Trondheim, Norway.

- Explicitly show how the ion exchange framework can yield a more oil-wet nature, as well as how pH influences this mechanism.
- Show a convenient experimental setup utilizing CO₂ buffering for pH control during low pressure waterflooding.

THEORY

Two much discussed mechanisms for wettability alterations during low salinity water flooding are the “expansion of the electrical double layer” and “cation exchange”. The two mechanisms will be reviewed herein with the aim of generalizing their effects.

Expansion of the Electrical Double Layer

An electric double layer is a dense, diffuse, layer of counter ions near a charged surface. A decreased salinity yields less screening, i.e., larger electrostatic forces between oil and mineral. In its simplest form one therefore only need to regard the sign of the net charge to predict whether a decreased salinity should yield stronger attraction (unequally charged) or stronger repulsion (equally charged) between oil and mineral. Table 1 gives a generalization of the most abundant minerals.

Table 1; The qualitative influence of net charge during decreasing salinity

Solid	Charge on solid	Charge on oil	Net effect in low salinity
Clays	Negative	Usually negative	Repulsion, i.e., more water-wet
Carbonates	Positive		Attraction, i.e., more oil-wet
Quartz	Negative		Repulsion, i.e., more water-wet

Adhesion tests [3] of the basic Minnelusa oil on Kaolinite, however, showed increased adhesion with decreasing salinity at pH 6 where both surfaces had net negative charge. Equivalent results have also been reported by e.g. Drummond and Israelachvili [4]. Hence to regard only the sign of the net charges is too simplistic an approach.

Ion Exchange

Ion exchange is a well-known phenomenon that essentially is a consequence of electrical double layers, and it is well described in the literature (see e.g., Appelo and Potsma [5]). Clays are particularly important for the ion exchange process since they have a large surface area and a large number of negatively charged exchange sites, i.e., a large cation exchange capacity (CEC). Generally, ions with higher charge density, i.e., higher valence or smaller hydrated radii, are preferentially adsorbed. This is normally described by an exchange reaction as given in Eq. 1.



K denotes the equilibrium constant for the reaction, c denotes concentration, X is the exchange site on the clay and β corresponds to the fraction of sites on the ion exchanger. Note that the ionic strength dependence of all K values was omitted for simplicity herein.

Due to the square root term the fraction of sites occupied by Ca^{2+} increases relative to Na^+ during dilution of a water of given $\text{Ca}^{2+}/\text{Na}^+$ ratio. Hence Ca^{2+} will be scavenged from solution by the ion exchanger. Figure 1 shows a typical observation (see, e.g., [7]) with the creation of a “shock front” with very low concentration of divalent ions, directly after the injection of the low salinity solution (6% SSW (Synthetic SeaWater) with $\sim 25\text{mg/l Ca}^{2+}$ and $\sim 77\text{mg/l Mg}^{2+}$). The low divalent concentrations are accompanied by a pH increase due to the water containing very little buffer capacity. Modeling with PHREEQC [10] showed that ion exchange alone could not explain the high pH. The “shock front” can, however, be fully explained by introducing equilibrium with a carbonate mineral like dolomite or calcite.

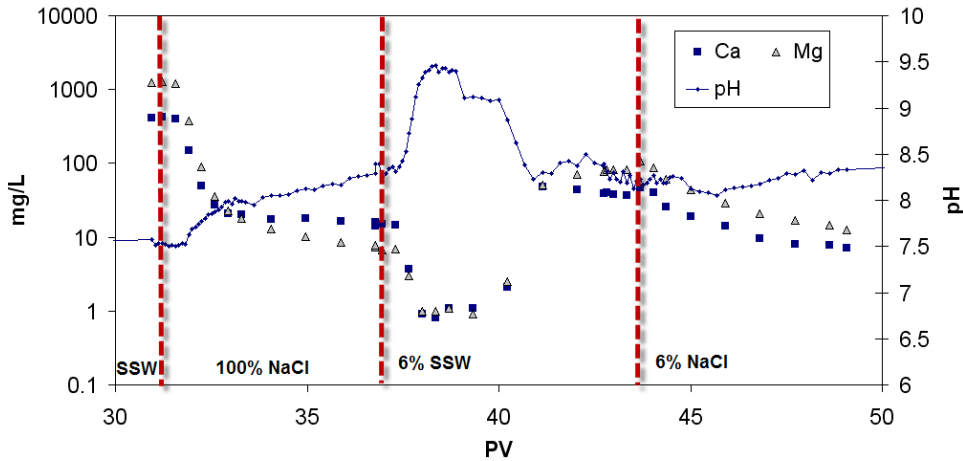


Figure 1: Measured Ca^{2+} and Mg^{2+} concentrations and pH from flooding of a Berea core [6]. SSW and NaCl denote synthetic seawater and pure sodium chloride brine respectively. 6% corresponds to a 6% dilution with distilled water.

Adsorption of Organic Species

Polar organic species can be included in an ion exchange model in the same manner as given for inorganic ions above. The present work regards two types of binding mechanisms, where the polar organic species were denoted *HA* (Acid) and *B* (Base) as illustrated in Figure 2. The former corresponds to “Cation bridging” and the latter to “Cation exchange” in the denotation used by Lager et.al. [2].

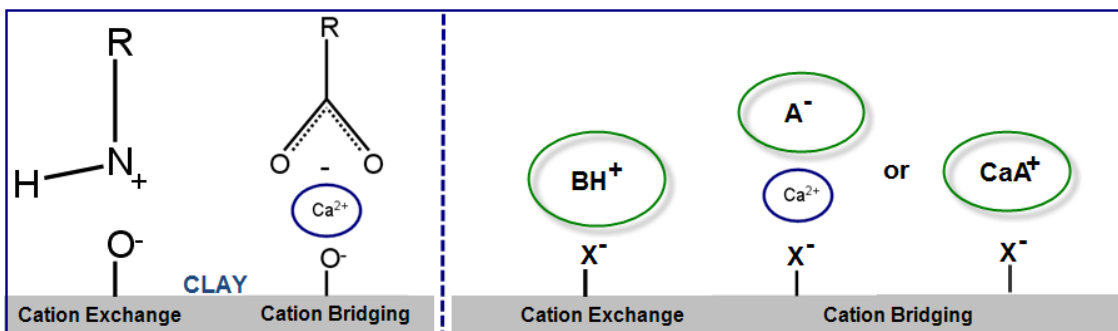


Figure 2; Example of two organic-clay binding mechanisms

Acids and bases are present as neutral species in the oil, but can partition into water and ionize as summarized in Table 2. The aqueous equilibria are common acid/base and complexing reactions that introduce the pH dependence of the organic-clay bonding.

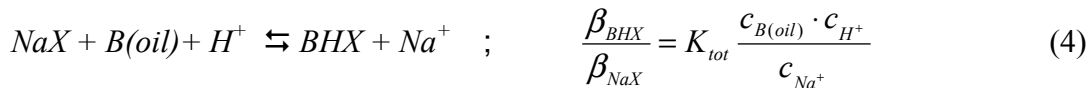
Table 2: Equilibria for the two types of organic-clay bonding.

	Cation exchange	Cation bridging
Oil/water partitioning	$B(oil) \rightleftharpoons B(aq); \quad K_{H-B} = \frac{c_B}{c_{B(oil)}}$	$HA(oil) \rightleftharpoons HA(aq); \quad K_{H-HA} = \frac{c_{HA}}{c_{HA(oil)}}$
Aqueous equilibria	$B+H^+ \rightleftharpoons BH^+; \quad K_B = \frac{c_{BH^+}}{c_B c_{H^+}}$	$HA \rightleftharpoons A^- + H^+; \quad K_A = \frac{c_{A^-} c_{H^+}}{c_{HA}}$ $A^- + Ca^{2+} \rightleftharpoons CaA^+; \quad K_{CaA} = \frac{c_{CaA^+}}{c_{A^-} c_{Ca^{2+}}}$

At the water/solid interface the “organic ions” can exchange with inorganic cations as Na^+ or Ca^{2+} ;



Eq. 2-3 show that decreasing concentrations of Na^+ and Ca^{2+} will shift the reactions to the right yielding more adsorption of the organic component BH^+ . Including the pH dependence of BH^+ yields Eq. 4, where $B(oil)$ denotes the concentration of basic components in the oil and K_{tot} corresponds to the equilibrium constant;



It should be noted that decreasing Na^+ shifts Eq. 4 in the opposite direction than increasing pH , i.e., decreasing H^+ . For the “Cation bridging” mechanisms it can similarly be shown that a decreased salinity yields desorption of organic molecules as summarized in Table 3.

Table 3: Influence of salinity and pH on the clay-organic bonding, detailed for Na^+ and Ca^{2+} .

Binding	Equilibria at solid surface		Reduced salinity	pH increase
Cation Exchange	$\frac{\beta_{BHX}}{\beta_{NaX}} \propto \frac{c_{H^+}}{c_{Na^+}}$	$\frac{\beta_{BHX}}{\sqrt{\beta_{CaX_2}}} \propto \frac{c_{H^+}}{\sqrt{c_{Ca^{2+}}}}$	Adsorption	Desorption
Cation Bridging	$\frac{\beta_{CaAX}}{\beta_{NaX}} \propto \frac{c_{Ca^{2+}}}{c_{Na^+} c_{H^+}}$	$\frac{\beta_{CaAX}}{\sqrt{\beta_{CaX_2}}} \propto \frac{\sqrt{c_{Ca^{2+}}}}{c_{H^+}}$	Desorption	Adsorption

Two important points should be noted from Table 3;

- Low salinity injection can alter wettability in both directions, i.e., either more water-wet (desorption), or more oil-wet (adsorption).
- A pH increase acts in the opposite direction of salinity reduction.

The latter statement is important as it can introduce a significant difference between reservoir and laboratory. In a reservoir the pH is buffered due to that acidic species like CO_2 are present. During low pressure core floods however, the system is usually unbuffered and the pH is consequently allowed to rise. It is emphasized that this pH increase may lead to false conclusions.

At a stable pH low salinity water should lead to less components being bound by “bridges” and more components being directly bound to the surface (cation exchange). This is consistent with the above mentioned adhesion tests [3,4]. Assuming that the two binding mechanisms shown in Figure 2 are dominating, one can generalize that acidic oils should yield more water-wet surfaces in low saline water (cation bridging), while basic oils should lead to more oil-wet surfaces (cation exchange). This generalization has been adapted as a working hypothesis in our lab. Its validity depends on pK_a and pK_b values of the polar components in the oil. Further discussion will not be given herein but RezaeiDoust et.al. [8] provide a good discussion concerning such values.

An Endicott field case [9] showed most interestingly that iron appeared in the produced water during low salinity flooding. In the high saline periods before and after the low saline injection iron was not detected. This was a strong indication that some kind of chelating compounds were present during low salinity flooding. Such compounds could either come from the oil directly or from material being detached from the solid surface. The latter explanation was used by Lager et.al. [9] and is consistent with detachment of “cation bridges” in the framework above. It is noted that this field case show similarities with the use of sodium citrate, i.e., a chelating agent, during core preparation [12].

EXPERIMENTAL

All water compositions as well as rock properties can be found in Table 4 and Table 5. An oil and condensate mix from a North Sea field was filtered (3 μm) and stabilized (1 atm) at 130 °C to yield the stock tank oil of Table 6 used in these experiments.

Core Preparation

Each core plug (3.8 cm diameter, 4.8 cm long) was cleaned by Toluene/Methanol flooding, and saturated with formation water (FW). Thereafter the plugs were drained in a centrifuge to obtain initial water saturation and aged for three weeks at 124°C and 7 bara. Oil permeability was measured before and after aging as well as after mounting of composites.

Core Flooding

All flooding experiments were performed vertically in a standard core flooding rig at 124°C and ~20 bara with a sleeve pressure of ~60 bara. A flooding rate of 8ml/h was chosen as a compromise in order to approximate typical reservoir velocities while limiting the time required to perform the experiments. Conductivity and pH was measured with inline meters at the outlet, while all aqueous solutions were kept under N₂ atmosphere to avoid oxygen ingress. Table 7 gives all core and composite properties.

Table 4: Aqueous compositions. All solutions filtered (0.45µm) and degassed prior to use.

Salt	FW g/l	SSW g/l	SSW5 g/l	NaCl2 g/l	SSW-CO ₂ * g/l	NaCl2-CO ₂ * g/l*
NaCl	35.01	23.74	1.19	0.82	23.74	0.35
CaCl ₂	3.01	1.13	0.06	0	1.13	0
MgCl ₂	0.22	5.01	0.25	0	5.01	0
KCl	0.76	0.76	0.04	0	0.76	0
Na ₂ SO ₄	0.00	3.98	0.20	0	3.98	0
NaHCO ₃	0.62	0.19	0.01	0	0.67	0.67
SrCl ₂	0.00	0.01	0.00	0	0.01	0
HAc	0.45	0	0	0	0	0
TDS	40075	34820	1741	820	35300	1022
I	0.71	0.69	0.035	0.014	0.70	0.014

*CO₂ saturated solutions @~1bara, ~25°C.

Table 5: X-ray diffraction(XRD) analysis of rock material.

Formation	XRD	Qtz	Kfsp	Plag	Chl	Kao	Mi/Il	ML	Sme	Cal	Sid	Dol	Pyr	Gyp
Rannoch Field G	Whole rock	42.9	16.7	15.6	1.0	8.8	7.6	0.9	0.2	0.0	5.0	1.0	0.2	0.0
	fine frac.<4µm	4.3	2.6	1.4	5.6	56.6	16.9	0.3	0.0	0.0	10.3	1.0	1.0	0.0
Rannoch Field V	Whole rock	23.6	9.7	8.5	3.3	32.7	12.3	0.6	0.1	0.0	7.6	1.0	0.6	0.0
	fine frac.<4µm	0.3	0.4	0.0	0.9	92.2	5.7	0.2	0.0	0.0	0.2	0.0	0.1	0.0

Table 6: Oil properties.

Parameter	value	Unit
TAN (Total Acid number)	<0.1	[mgKOH/g]
TBN (Total Base Number)	0.28	[mgKOH/g]
Asphaltenes	0.7	[wt%]
Wax	4.8	[wt%]
IEP (Iso electric point)	3.5 (@500ppm NaCl) 2.6(@5000ppm NaCl)	[pH]
Density @20°C	0.8160	[g/ml]
Viscosity@20°C, 1bara	2.27	[cP]
Viscosity@124°C, 20 bara	0.53	[cP]

Kfsp	K-feldspar
Plag	Plagioclase
Chl	Chlorite
Kao	Kaolinite
Mie/Il	Mica and illite
ML	Mixed Layer Clay
Smect	Smectite
Calc	Calcite
Sid	Siderite
Dol/Ank	Dolomite and Ankerite
Pyr	Pyrite

Table 7: Individual and composite core data from Field G of Table 5.

Core ID	Experiment G1		Experiment G2			Experiment G3	
	A	B	C	D	E	F	G
Length (cm)	4.81	4.79	4.80	4.80	4.80	4.80	4.80
Diameter (cm)	3.80	3.80	3.80	3.80	3.80	3.80	3.80
Pore volume (cm ³)	11.60	11.20	15.0	14.90	14.80	11.40	11.80
Porosity (frac.)	0.21	0.21	0.28	0.27	0.27	0.21	0.22
Water permeability, kw (mD)	90.9	69.7	158	147	147	74.3	80.2
Swi (frac.)	0.16	0.16	0.15	0.14	0.14	0.12	0.17
Ko(Swi) before ageing (mD)	83.4	62.6	146	135	131	66.8	71.0
Ko(Swi) after ageing (mD)	87.4	67.2	144	146	141	73.5	78.1
Composite length (cm)	9.60		14.4			9.60	
Composite pore volume (cm ³)	22.9		44.6			23.2	
Composite Swi	0.16		0.14			0.15	
Composite Ko(Swi) (mD)	78.0		149			76.0	

RESULTS AND DISCUSSION

Figure 3 shows a comparison of the remaining oil saturation (ROS) from the initial part of three flooding experiments on the core material shown in Table 7. In the displayed time interval Experiment G1 is a standard high-salinity flood, Experiment G3 is a secondary low-salinity flood, while Experiment G2 changes from high to low salinity after approximately 2.5 Pore Volumes Injected (PVI). It should be noted that the secondary low-salinity flood has lower water saturation at breakthrough and less production than the other two floods, and that in Experiment G2 the oil production stops with the introduction of low-salinity water.

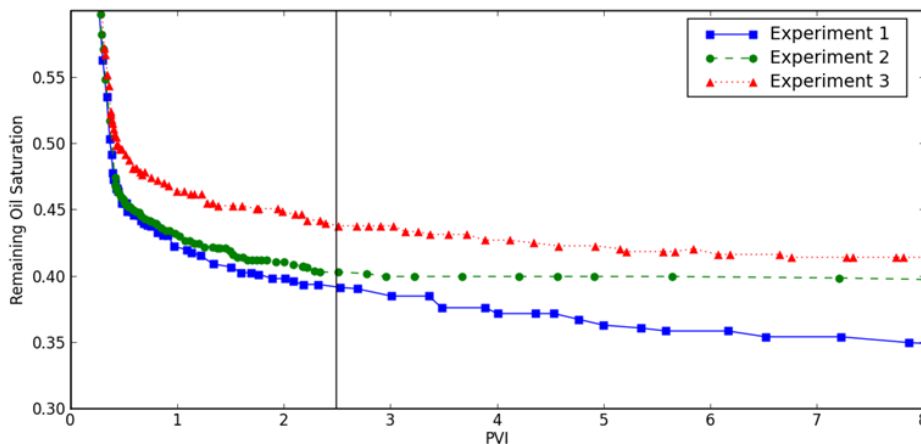


Figure 3: Remaining oil saturation in the initial parts of Experiment 1-3. Experiment 1 was a standard high-salinity flood, while in Experiment 2 the salinity was changed from high (SSW) to low(SSW5) at ~2.5 PVI. Experiment 3 was a secondary low-salinity flood.

When presenting that ‘low-salinity injection stops oil production’, we need to emphasize that these were relatively low rate experiments on composite cores. Hence, the results were susceptible to capillary end effects, not only at the outlet, but also at the internal interfaces due to poor capillary contact. Effectively, this laboratory artefact may cause the

end-face saturations to be pinned at the values where the capillary pressure is zero, which effects the entire saturation distribution (see, e.g., Huang and Honarpour [14]).

To account for end effects, the secondary flooding experiments (Experiment G1 and G3) were history-matched using the low-salinity functionality in Eclipse 100 [15] to obtain estimates of the relative permeability and capillary pressure curves for high and low salinity water injection. The experimental and history-matched data are shown in Figure 4 and Figure 5, while the estimated flow functions are shown in Figure 6. Using these curves ‘as-is’ in a simulation of Experiment G2 the qualitative behaviour was reproduced as shown in Figure 7[†].

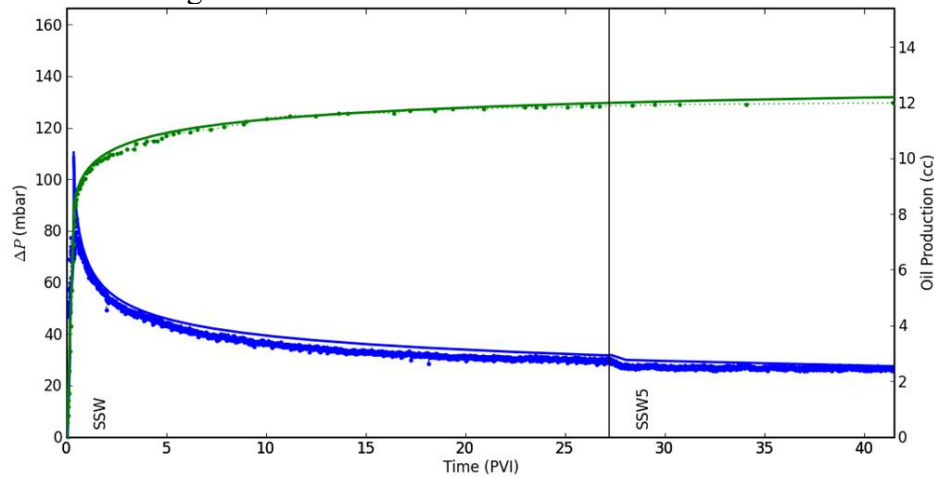


Figure 4: Experimental (dotted) and simulated (solid) data for Experiment G1. The upper lines show oil production and the lower lines show the pressure drop across the core.

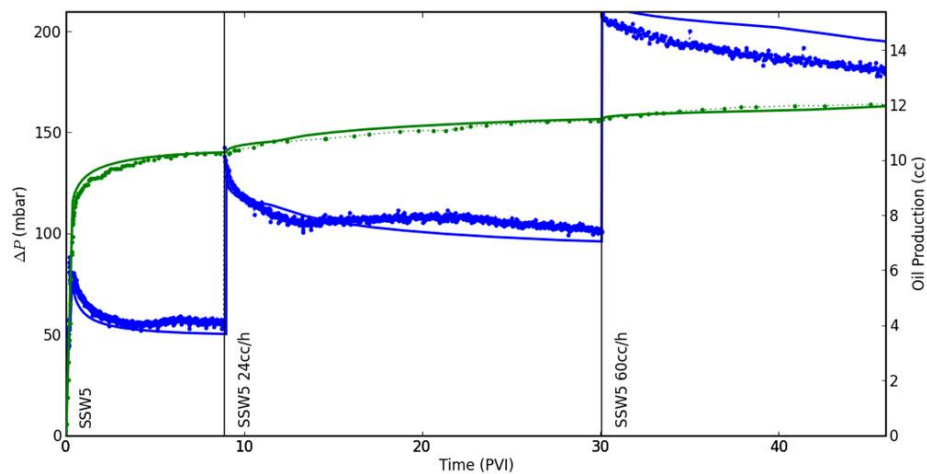


Figure 5: Experimental (dotted) and simulated (solid) data for Experiment G3.

[†] This indicates that the qualitative shift in the flow functions is consistent although the cores used in experiment G2 have slightly different properties than those of experiments G1 and G3.

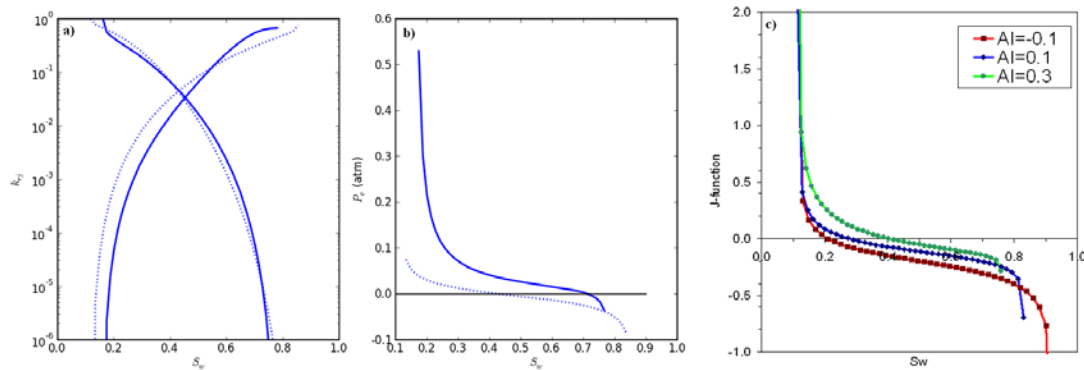


Figure 6: a) Relative permeability and b) P_c . Both estimated from secondary high-salinity (solid) and low-salinity (dotted) experiments. c) Imbibition capillary pressure for three different Amott indices estimated by pore network modelling.

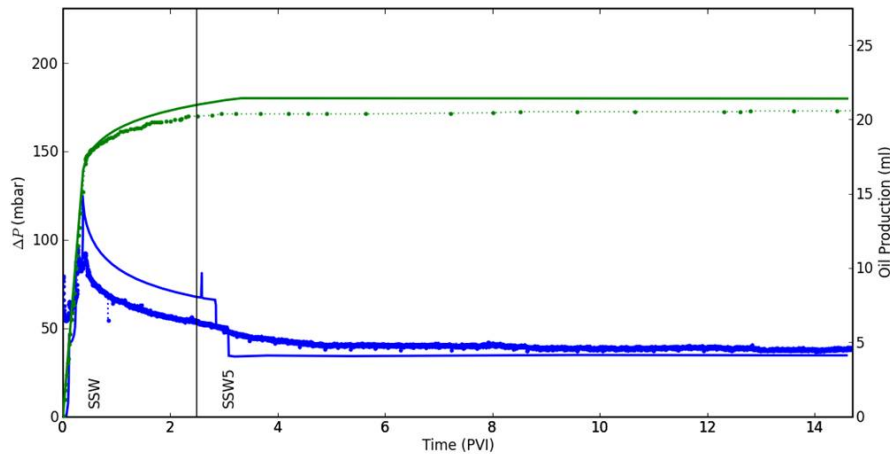


Figure 7: Experimental data (dotted) for Experiment G2, along with simulation (solid) using parameters estimated from Experiments G1 and G3.

Without separately measured capillary pressure data or in-situ saturation monitoring the parameter estimation is poorly constrained, and the uncertainties are large. However, in order to approximate the experimental results, the low-salinity capillary pressure curve needs to be significantly shifted down compared to the high-salinity curve. Such a shift is an indication of a wettability alteration towards more oil-wet conditions. Furthermore, the lower water saturation at breakthrough and lower total recovery for the secondary low-salinity flood are also indications of increased oil-wetness.

In an attempt to reduce the uncertainty a pore network model was constructed using commercial technology [13]. Imbibition capillary pressures were subsequently estimated for different wettability scenarios. Results for three different values of the Amott Index (AI) are shown in Figure 6c). The network model has not been tuned to the experimental data, but the results show that for this core material, a significant shift in capillary pressure is possible by a moderate change in wettability.

When wettability is altered from water-wet conditions in the more oil-wetting direction, a typical behaviour is that the residual oil saturation decreases. This has been shown experimentally by Jadunandan and Morrow [16] and by using pore-scale modelling [17,18]. From the interpretation above it is also the case for the present experiments even though the end-effect artefact actually reduces the observed production. The pore-modelling explanation for the ‘residual oil versus wettability’ trend is that increased oil wetting increases the amount of connected oil films, allowing more oil to be drained at low saturations. Once the films have collapsed it is less likely that a wettability alteration can re-establish connectivity, hence the point at which low-salinity water is injected will be important for the result. In Experiment G1 low-salinity water was injected after more than 25 PVI of high-salinity injection and no response was observed other than the expected pressure drop due to the density and viscosity differences (See Figure 4).

Why Did The Rock Become More Oil Wet?

As shown above the observation of a more oil-wet surface corresponds with the ion exchange framework for the basic oil used herein. However, because oil contaminated the inline pH meter yielding drift in the results it was not possible to measure the pH. To verify the hypothesised mechanism it is therefore needed to run the same experimental series with pH control. Preferably with a CO₂ buffered system as proposed below. The other likely explanation is that the relatively high amounts of siderite (FeCO₃) plays a role. Low salinity should, as described above, lead to a stronger binding between the positive carbonate surface and the net negative oil. Iron ions are in addition surface active and can significantly alter the surface potential at ppm concentrations [12], hence the presence of iron could have significantly altered the surface-potential of the clay. The latter possibility should be detectable by proper zeta-potential measurements. Figure 8 shows cryoESEM pictures of the situation after the low salinity flooding. The remaining oil is clearly associated with both the siderite and the clay, i.e., it was not possible to differentiate between the possible explanations based on these pictures.

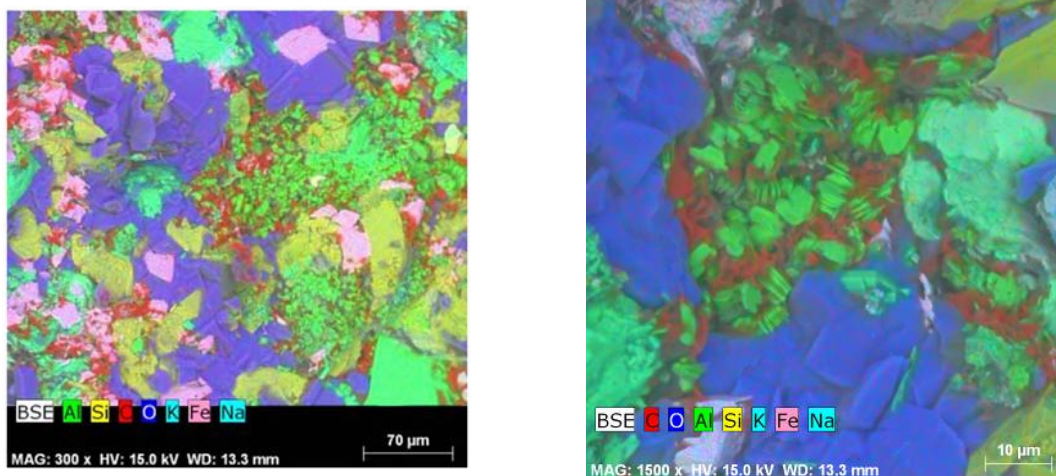
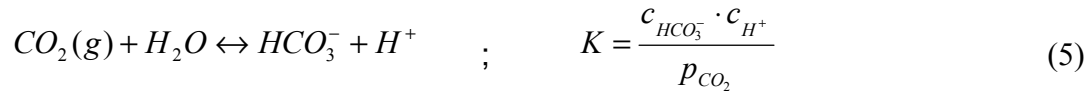


Figure 8: CryoESEM(cryogenic Environmental Scanning Electron Microscopy) images showing the end distribution of oil (red) and water (blue) for the G2 experiment. Kaolinite is presented with green colour, iron-rich carbonate cement as pink and Quartz as yellow.

The Use of CO₂ Buffering In Low Pressure Core Floods

CO₂ is often the acidic specie that controls pH in an oil field reservoir. The pH value is in such cases determined by bicarbonate (HCO_3^-) concentration and CO₂ pressure as given by Eq. 5. Bicarbonate concentration in water samples is routinely analysed by alkalinity titration, but further description of the alkalinity concept [11] will not be given herein.



It is simply noted that the presence of this buffer system is a major difference between reservoir conditions and experiments at reduced conditions. To eliminate this potential artefact during low pressure core floods a simple experimental setup was tested where all the injection waters contained the same bicarbonate/CO₂ ratio (see Table 4). This was achieved by equilibrating the waters with CO₂(g) at ambient conditions (~1atm, ~25°C). Figure 9 shows that the CO₂ buffer efficiently controlled the pH. It is emphasized that the proposed buffer system is not an attempt of directly mimicking the reservoir, but a convenient method to eliminate the pH effect during mechanistic studies. This approach should provide further insight into the low salinity mechanisms, but care must be taken if comparing floods performed with and without CO₂ buffering. This is due to that a few percent CO₂ partitions into the oil and thereby alters its properties.

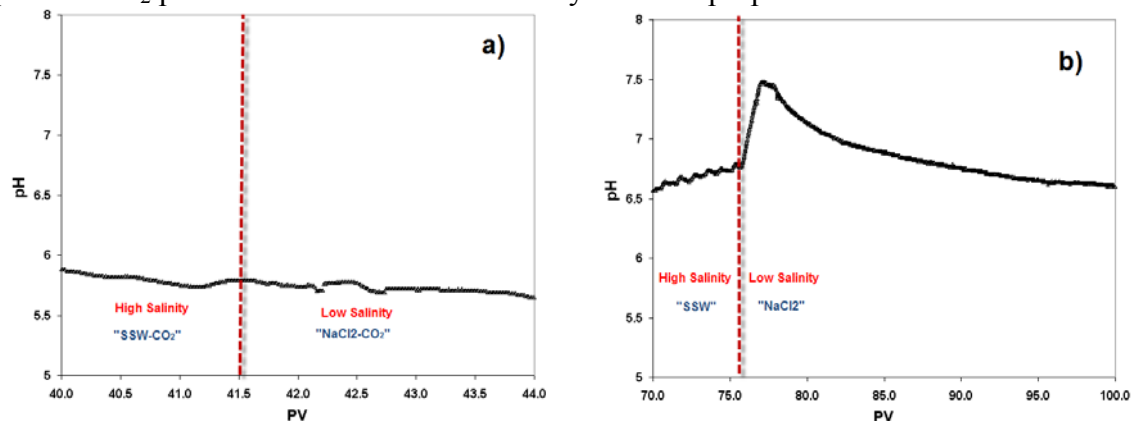


Figure 9: Outlet pH of a core from Field V (see Table 5) during low salinity injection (see Table 4). a) CO₂ saturated solutions. b) Solutions under N₂ atmosphere.

CONCLUSIONS

During core floods on a sandstone from the Norwegian Continental Shelf (NCS) it was observed that the introduction of low salinity water yielded a halt in oil production. This can be explained by capillary end effects and a significant shift in the capillary pressure curve that is consistent with a wettability alteration towards more oil-wet conditions. Pore-scale modelling was used to demonstrate that a moderate change in wettability can induce a significant shift in the capillary pressure for this rock material. Loss of oil film continuity can explain why a significant change only occurred when low-salinity water was introduced early in the flooding.

The ion exchange mechanism was reviewed to show that it can account for wettability alteration in both directions, depending on oil and rock properties. A pH increase acts in the opposite direction of a decreased salinity. This may lead to artefacts in low pressure core floods, hence a simple CO₂ system was proposed as a convenient method to eliminate this pH uncertainty. The efficiency of the CO₂ buffer system was experimentally demonstrated.

ACKNOWLEDGMENT

We would like to thank Ole Jakob Arntzen for valuable discussions and Tony Boassen for taking the cryoESEM pictures.

REFERENCES

1. Ligthelm, D.J., J. Gronsveld, J.P. Hofman, N.J. Brussee, and H.A. Van der Linde, "Novel Waterflooding Strategy By Manipulation Of Injection Brine Composition." *SPE 119835, SPE/EAGE, Amsterdam, Netherlands, (8-11 June 2011)*
2. Lager, A., K.J. Webb, C.J.J. Black, M. Singleton, K.S. Sorbie, "Low salinity oil recovery: An experimental investigation," *Int. Symp. of the SCA*, (2006)
3. Lebedeva, E.V. and A. Fogden, "Adhesion of Oil to Kaolinite in Water", *Environ. Sci. Technol.* (2010), **44**, 9470–9475
4. Drummond, C. and J. Israelachvili, "Surface forces and Wettability" *Journal of Petroleum Science and Engineering*, (2002), **33**, 123– 133
5. Appelo, C.A.J. and D. Postma, *Geochemistry, groundwater and pollution, 2nd ed.*, Third corrected reprint, Balkema, (2007), ISBN-04-1536-421-3.
6. Wideroe, H.C., H. Rueslaatten, T. Boassen, C.M. Crescente, M. Røphaug, G.H. Soerland, H. Urkedal, "Investigation of Low salinity water flooding by NMR and CryoESEM", *Int. Symp. of the SCA, Halifax, Canada* (2010)
7. Cissokho, M., S. Boussour, Ph. Cordier, H. Bertin, G. Hamon, "Low salinity oil recovery on clayey sandstone: experimental study", *Int. Symp. of the SCA*, (2009)
8. RezaeiDoust, A., T. Puntervold, T. Austad, "Chemical verification of the EOR mechanism by using low saline/smart water in sandstone" *Energy and Fuels*, (2011), **25**, 2151-2162
9. Lager, A., K. Webb, J. Seccombe, "Low salinity waterflood, Endicott, Alaska, Geochemical Study & Field evidence of multicomponent Ion Exchange", *EAGE IOR symposium, Cambridge*, (2011)
10. Parkhurst, D.L. and C.A.J. Appelo, *User's guide to PHREEQC (version 2)*, (1999)
11. Kaasa, B. and T. Østvold, "What Alkalinity is and How it is Measured", *SPE 37277 Int. Symp. Oil field scale, Houston, Texas*, (1997)
12. Rueslåtten, H.G., O. Hjelmeland, O.M. Selle, "Wettability of reservoir rocks and the influence of organo-metallic compounds", *North sea oil and gas reservoirs.*, (1994), **3**, 317-324
13. <http://www.numericalrocks.com>; accessed 28.04.2011
14. Huang, D.D. and M.M. Honarpour, "Capillary End Effects in Coreflood Calculations", SCA1996-34, *Int. Symp. of the SCA.*, (1996)
15. Schlumberger, Eclipse Simulation Software Manuals 2010.2, (2010)
16. Jadhunandan P.P. and N.R. Morrow "Effect of Wettability on Waterflood Recovery for Crude-Oil/Brine/Rock Systems", SPE 22597, *SPE Reservoir Engineering*, (1995)
17. Øren, P-E. and S. Bakke, "Reconstruction of Berea Sandstone and Pore-Scale Modelling of Wettability Effects", *J. of Petroleum Science and Eng.*, (2003), **39**, 177-199.
18. Zhao, X., M.J. Blunt and J. Yao, "Pore-Scale Modelling: Effects of Wettability on Waterflood Oil Recovery", *J. of Petroleum Science and Eng.*, (2010), **71**, 169-178.